

# QCD predictions of heavy quark production at RHIC\*

R. Vogt<sup>a,b</sup>, M. Cacciari<sup>c</sup> and P. Nason<sup>d</sup>

<sup>a</sup>Lawrence Berkeley National Laboratory, Berkeley, CA USA

<sup>b</sup>Physics Department, University of California, Davis, CA USA

<sup>c</sup>LPTHE, Université Pierre et Marie Curie (Paris 6), France

<sup>d</sup>INFN, Sezione di Milano, Italy

We make up-to-date QCD predictions for heavy flavor production in  $\sqrt{S} = 200$  GeV  $pp$  collisions at RHIC. We also calculate the electron spectrum from heavy flavor decays to directly compare to the data. A rigorous benchmark, including the theoretical uncertainties, is established against which nuclear collision data can be compared to obtain evidence for dense matter effects.

Recent improvements in heavy quark production theory and experimental measurements at colliders, especially for bottom production, have shown that the perturbative QCD framework seems to work rather well, see Refs. [1,2]. It is important to continue to validate this theoretical framework and its phenomenological inputs, extracted from other measurements, with new data such as that obtained at RHIC by PHENIX [3] and STAR [4,5]. Comparison of the  $pp$  and d+Au data  $\sqrt{S_{NN}} = 200$  GeV with theoretical benchmark calculations will aid in the interpretation of heavy flavor production in nucleus-nucleus collisions. Thus up-to-date benchmark calculations of both the total charm yield and the transverse momentum spectra are imperative.

We calculate the transverse momentum ( $p_T$ ) distributions of charm and bottom quarks, the charm and bottom hadron distributions resulting from fragmentation and, finally, the electrons produced in semi-leptonic decays of the hadrons [6]. At each step, we clarify the theoretical framework as well as the parameters and phenomenological inputs. Theoretical uncertainties are estimated as extensively as possible. Our final prediction is thus not a single curve but rather an uncertainty band which has a reasonably large probability of containing the ‘true’ theoretical prediction.

The theoretical prediction of the electron spectrum includes three main components: the  $p_T$  and rapidity distributions of the heavy quark  $Q$  in  $pp$  collisions at  $\sqrt{S} = 200$  GeV, calculated in perturbative QCD; fragmentation of the heavy quarks into heavy hadrons,  $H_Q$ , described by phenomenological input extracted from  $e^+e^-$  data; and the decay of  $H_Q$  into electrons according to spectra available from other measurements. This cross section

---

\*This work was supported in part by the Director, Office of Energy Research, Division of Nuclear Physics of the Office of High Energy and Nuclear Physics of the U. S. Department of Energy under Contract No. DE-AC02-05CH11231.

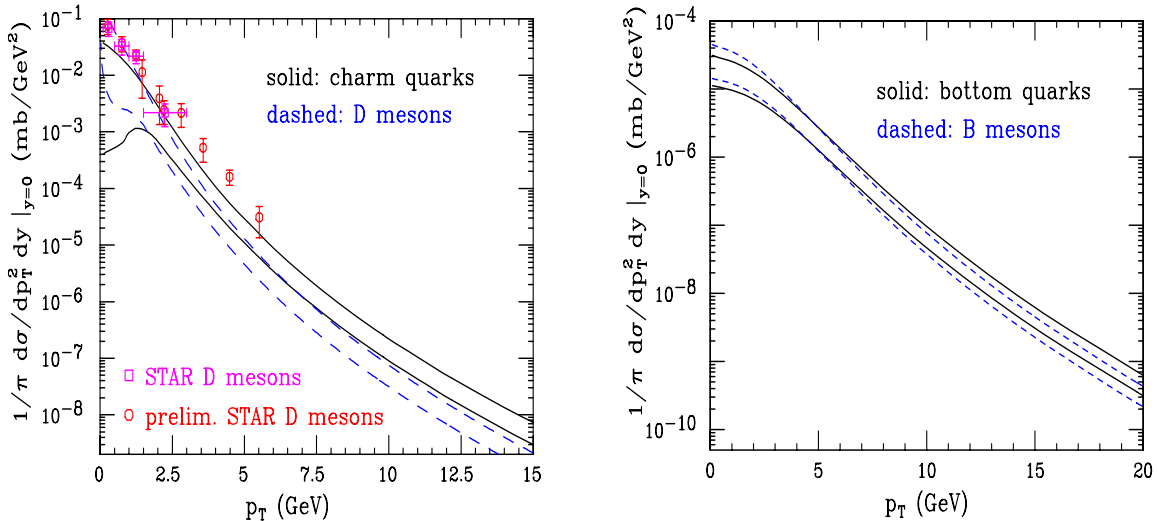


Figure 1. Left-hand side: The theoretical uncertainty bands for  $c$  quark and  $D$  meson  $p_T$  distributions in  $pp$  collisions at  $\sqrt{S} = 200$  GeV, using  $\text{BR}(c \rightarrow D) = 1$ . The final [4] and preliminary [5] STAR d+Au data (scaled to  $pp$  using  $N_{\text{bin}} = 7.5$ ) are also shown. Right-hand side: The same for  $b$  quarks and  $B$  mesons.

is schematically written as

$$\frac{Ed^3\sigma(e)}{dp^3} = \frac{E_Q d^3\sigma(Q)}{dp_Q^3} \otimes D(Q \rightarrow H_Q) \otimes f(H_Q \rightarrow e) \quad (1)$$

where the symbol  $\otimes$  denotes a generic convolution. The electron decay spectrum,  $f(H_Q \rightarrow e)$ , accounts for the branching ratios.

The distribution  $Ed^3\sigma(Q)/dp_Q^3$  is evaluated at Fixed-Order plus Next-to-Leading-Log (FONLL) level, implemented in Ref. [7]. In addition to including the full fixed-order NLO result [8,9], the FONLL calculation also resums [10] large perturbative terms proportional to  $\alpha_s^n \log^k(p_T/m)$  to all orders with next-to-leading logarithmic (NLL) accuracy (i.e.  $k = n, n - 1$ ) where  $m$  is the heavy quark mass. The perturbative parameters are  $m$  and the value of the strong coupling,  $\alpha_s$ . We take  $m_c = 1.5$  GeV and  $m_b = 4.75$  GeV as central values and vary the masses in the range  $1.3 < m_c < 1.7$  GeV for charm and  $4.5 < m_b < 5$  GeV for bottom to estimate the mass uncertainties. The five-flavor QCD scale is the CTEQ6M value,  $\Lambda^{(5)} = 0.226$  GeV. The perturbative calculation also depends on the factorization ( $\mu_F$ ) and renormalization ( $\mu_R$ ) scales. The scale sensitivity is a measure of the perturbative uncertainty. We take  $\mu_{R,F} = \mu_0 = \sqrt{p_T^2 + m^2}$  as the central value and vary the two scales independently within a ‘fiducial’ region defined by  $\mu_{R,F} = \xi_{R,F}\mu_0$  with  $0.5 \leq \xi_{R,F} \leq 2$  and  $0.5 \leq \xi_R/\xi_F \leq 2$  so that  $\{(\xi_R, \xi_F)\} = \{(1,1), (2,2), (0.5,0.5), (1,0.5), (2,1), (0.5,1), (1,2)\}$ . The envelope containing the resulting curves defines the uncertainty. The mass and scale uncertainties are added in quadrature.

These inputs lead to a FONLL total  $c\bar{c}$  cross section in  $pp$  collisions of  $\sigma_{c\bar{c}}^{\text{FONLL}} = 256_{-146}^{+400} \mu\text{b}$  at  $\sqrt{S} = 200$  GeV. The theoretical uncertainty is evaluated as described above. The corresponding NLO prediction is  $244_{-134}^{+381} \mu\text{b}$ . The predictions in Ref. [11], using  $m_c = 1.2$  GeV and  $\mu_R = \mu_F = 2\sqrt{p_T^2 + m^2}$  gives  $\sigma_{c\bar{c}}^{\text{NLO}} = 427 \mu\text{b}$ , within the

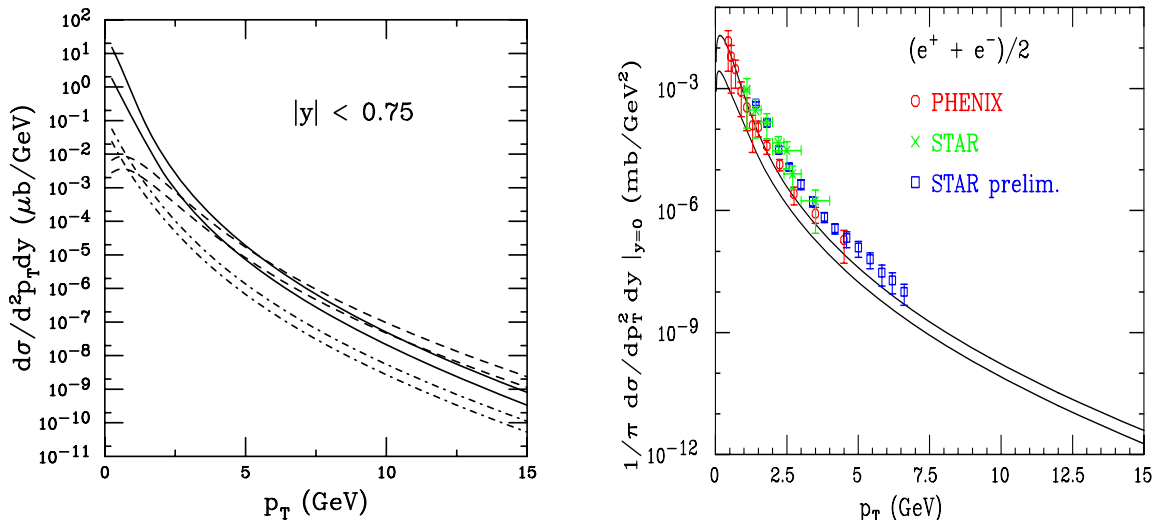


Figure 2. Left-hand side: The theoretical uncertainty bands for  $D \rightarrow e$  (solid),  $B \rightarrow e$  (dashed) and  $B \rightarrow D \rightarrow e$  (dot-dashed) as a function of  $p_T$  in  $\sqrt{S} = 200$  GeV  $pp$  collisions for  $|y| < 0.75$ . Right-hand side: The final electron uncertainty band in  $pp$  collisions is compared to the PHENIX [3] and STAR (final [4] and preliminary [5]) data.

uncertainties. Since the FONLL and NLO calculations tend to coincide at small  $p_T$ , which dominates the total cross section, the two results are very similar. Thus the two calculations are equivalent at the total cross section level, within the large perturbative uncertainties. The total cross section for bottom production is  $\sigma_{bb}^{\text{FONLL}} = 1.87^{+0.99}_{-0.67} \mu\text{b}$ .

The fragmentation functions,  $D(c \rightarrow D)$  and  $D(b \rightarrow B)$ , where  $D$  and  $B$  indicate a generic admixture of charm and bottom hadrons, are consistently extracted from  $e^+e^-$  data in the context of FONLL [12]. Using the Peterson *et al.* fragmentation function [13], with standard parameter choices  $\epsilon_c \simeq 0.06 \pm 0.03$  and  $\epsilon_b \simeq 0.006 \pm 0.003$  does not provide a valid description of fragmentation in FONLL.

The measured spectra for primary  $B \rightarrow e$  and  $D \rightarrow e$  decays are modeled and assumed to be equal for all bottom and charm hadrons, respectively. The contribution of electrons from secondary  $B$  decays,  $B \rightarrow D \rightarrow e$ , was obtained by convoluting the  $D \rightarrow e$  spectrum with a parton-model prediction of  $b \rightarrow c$  decay. The resulting electron spectrum is very soft, giving a negligible contribution to the total. The decay spectra are normalized using the branching ratios for bottom and charm hadron mixtures [14]:  $\text{BR}(B \rightarrow e) = 10.86 \pm 0.35\%$ ,  $\text{BR}(D \rightarrow e) = 10.3 \pm 1.2\%$ , and  $\text{BR}(B \rightarrow D \rightarrow e) = 9.6 \pm 0.6\%$ .

The left-hand side of Fig. 1 shows the theoretical uncertainty bands for  $c$  quarks and  $D$  mesons, obtained by summing the mass and scale uncertainties in quadrature. The band is broader at low  $p_T$  due to the large value of  $\alpha_s$  and the behavior of the CTEQ6M parton densities at low scales as well as the increased sensitivity of the cross section to the charm quark mass. The rather hard fragmentation function causes the  $D$  meson and  $c$  quark bands to separate only at  $p_T > 9$  GeV. The right-hand side of Fig. 1 shows the same results for  $b$  quarks and  $B$  mesons. The harder  $b \rightarrow B$  fragmentation function causes the two bands to partially overlap until  $p_T \simeq 20$  GeV.

Figure 2 shows the individual uncertainty bands for the  $D \rightarrow e$ ,  $B \rightarrow e$  and  $B \rightarrow D \rightarrow e$

decays to electrons on the left-hand side and compares the RHIC data to the total band on the right-hand side. The upper and lower limits of the band are obtained by summing the upper and lower limits for each component. The secondary  $B \rightarrow D \rightarrow e$  spectrum is extremely soft, only exceeding the primary  $B \rightarrow e$  decays at  $p_T < 1$  GeV. It is always negligible with respect to the total yield. While, for the central parameter sets, the  $B \rightarrow e$  decays begin to dominate the  $D \rightarrow e$  decays at  $p_T \simeq 4$  GeV, a comparison of the bands shows that the crossover may occur over a rather broad range of electron  $p_T$ . The relative  $c$  and  $b$  decay contributions may play an important part in understanding the electron  $R_{AA}$  in nucleus-nucleus collisions [15,16] which seems to suggest strong energy loss effects on heavy flavors [17,18].

We have presented theoretical uncertainty bands for heavy quarks, mesons and their electron decay products as a function of  $p_T$  in  $\sqrt{S} = 200$  GeV  $pp$  collisions at RHIC. These results should not be multiplied by any  $K$  factor. Rather, agreement within the uncertainties of the data would support the applicability of perturbative QCD to heavy quark production at RHIC. Significant disagreement would suggest that this evaluation needs to be complemented by further ingredients.

## REFERENCES

1. M. Cacciari, arXiv:hep-ph/0407187.
2. M. L. Mangano, arXiv:hep-ph/0411020.
3. S. S. Adler *et al.* [PHENIX Collaboration], arXiv:hep-ex/0508034.
4. J. Adams *et al.* [STAR Collaboration], arXiv:nucl-ex/0407006.
5. A. Tai [STAR Collaboration], J. Phys. G **30** (2004) S809 [arXiv:nucl-ex/0404029].
6. M. Cacciari, P. Nason and R. Vogt, Phys. Rev. Lett. **95** (2005) 122001 [arXiv:hep-ph/0502203].
7. M. Cacciari, M. Greco and P. Nason, JHEP **9805** (1998) 007 [arXiv:hep-ph/9803400]; M. Cacciari, S. Frixione and P. Nason, JHEP **0103** (2001) 006 [arXiv:hep-ph/0102134].
8. P. Nason, S. Dawson and R. K. Ellis, Nucl. Phys. B **303** (1988) 607; P. Nason, S. Dawson and R. K. Ellis, Nucl. Phys. B **327** (1989) 49 [Erratum B **335** (1990) 260].
9. W. Beenakker, W. L. van Neerven, R. Meng, G. A. Schuler and J. Smith, Nucl. Phys. B **351** (1991) 507.
10. M. Cacciari and M. Greco, Nucl. Phys. B **421** (1994) 530 [arXiv:hep-ph/9311260].
11. R. Vogt, Int. J. Mod. Phys. E **12** (2003) 211 [arXiv:hep-ph/0111271].
12. M. Cacciari and P. Nason, Phys. Rev. Lett. **89** (2002) 122003 [arXiv:hep-ph/0204025].
13. C. Peterson, D. Schlatter, I. Schmitt and P. M. Zerwas, Phys. Rev. D **27** (1983) 105.
14. S. Eidelman *et al.* [Particle Data Group Collaboration], Phys. Lett. B **592** (2004) 1.
15. J. Bielcik [STAR Collaboration], these proceedings.
16. S. A. Butsyk [PHENIX Collaboration], these proceedings.
17. M. Djordjevic, these proceedings.
18. N. Armesto, these proceedings.